Data processing at The South African Nuclear Energy Corporation SOC Ltd (Necsa) neutron diffraction facility

D Marais[1,2], A M Venter[1] and J Markgraaff[2]

[1] Research and Development Division, Necsa SOC Limited, PO Box 582, Pretoria, 0001, South Africa
[2] School of Mechanical and Nuclear Engineering, North-West University, Potchefstroom, 2520, South Africa

E-mail: deon.marais@necsa.co.za

Abstract. This paper describes the automated data treatment and reduction procedures developed for selected neutron diffraction instruments at Necsa as implemented in the software ScanManipulator. Examples of output data are illustrated for temperature dependent crystal structure investigations of an alumina powder, as well as depth-resolved d-spacing maps inside a welded mild steel sample.

1. Introduction

1.1. Neutron diffraction principle

Angular-dispersive neutron diffraction instruments utilize the principle that monochromatic thermal neutrons of wavelength λ are scattered coherently from the regular d_{hkl} spacing of crystalline planes in the material microstructure at angles θ_{hkl} given by the Bragg-law of diffraction, $2d_{hkl}sin\theta_{hkl} = \lambda$. Monochromatic thermal neutrons can be obtained from fission-spectrum neutrons produced in a steady-state nuclear reactor by placing neutron optical elements such as filters, monochromators and collimators in the neutron flight path. When directing a monochromatic neutron beam onto a crystalline sample, neutrons will be scattered as a distribution of Debye-Scherrer cones of varying apex angles centered on the beam axis. The apex angles can be precisely determined with neutron detectors positioned around the sample.

Efficient instrument performance is achieved through the use of neutron area detectors that enable intercepts with large sections of the Debye-Scherrer cones. This renders improved statistics and reduced measurement time. Ideally, the detector should be spherical and centered on the sample. This is however technically very challenging and financially taxing. As a compromise, arrays of flat detectors are generally used provided that relevant corrections are performed.

1.2. Data treatment and reduction software

A number of software packages are available which apply the necessary correction and reduction algorithms to raw diffraction data, GumTree [1] and Mantid [2] serving as examples. These packages tend to be large frameworks which cater for a broad spectrum of data treatment requirements, but with limited international standardization on the data acquisition and control (DAC) protocols between diffraction instruments, the software is generally not directly compatible with all instrument

modalities. This requires independent adaptation of existing third party software which could become very cumbersome.

1.3. The Necsa neutron diffraction facility(NDIFF)

The NDIFF at the SAFARI-1 research reactor of the South African Nuclear Energy Corporation (Necsa) SOC Limited has recently been upgraded with the aim to provide the African research community with neutron diffraction instrumentation of international stature. These instruments include a powder diffractometer named PITSI and a residual strain scanner named MPISI. With this upgrade, solutions were required to facilitate data acquisition, reduction and processing.

For DAC Necsa has standardized on the Australian Nuclear Science and Technology Organization (ANSTO) version of the SINQ Instrument Control Software (SICS) [3] on both instruments. Since MPISI is similar to ANSTO's Kowari neutron strain scanner, data reduction and processing can be performed with the Kowari customization of GumTree. However, since the PITSI detector geometry is not supported by GumTree, substantial modifications would be required to establish a compatible data reduction environment. With GumTree being a very expansive framework this implied a steep learning curve that had to be overcome before additions and modifications could be made. This is also true for other diffraction data processing frameworks such as Mantid. It was therefore decided to create the built-for-purpose software, ScanManipulator, to address instrument specific requirements.

Figure 1 schematically depicts the data treatment modalities implemented for PITSI to facilitate corrections, integration, normalization and stitching of data taken at a number of detector angles to render a final diffraction pattern. With the detector of PITSI only covering 20° in 2θ, a full diffraction pattern covering $9° \leq 2\theta \leq 116°$ in angular extent needs to be compiled from sequential positioning of the detector to at least seven different 2θ angles (frames) and allowing approximately 4° overlap between frames for the stitching process.

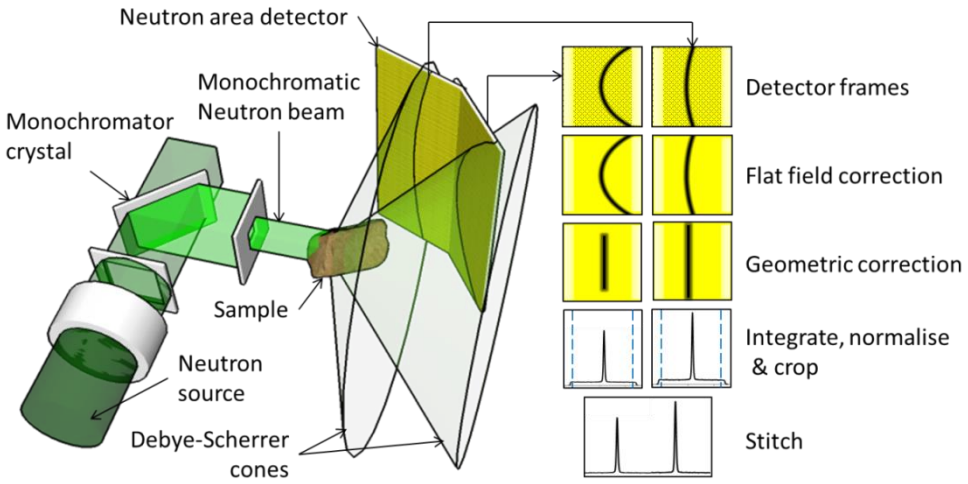

Figure 1. Illustration of an angular-dispersive neutron diffractometer geometry as well as the data correction and reduction steps required to produce a diffraction pattern from individual detector frames.

2. ScanManipulator

2.1. Implementation language.

ScanManipulator was implemented with the scripting language Python with the visual interface created with PyQt, making it a cross-platform application. It relies extensively on the scientific computing package Numpy for array manipulation and a number of third-party open-source libraries which provide the following functionalities:

- PySpec performs function fitting through regression techniques. It is used in analysis of X-ray diffraction data produced by the SPEC X-Ray Diffraction and Data Acquisition software [4].
- H5py access binary HDF5 datasets which is a primary storage mechanism of SICS [5].
- Matplotlib [6] is used to display 2D data and Mayavi [7] to display 3D data.

2.2. Data treatment and reduction functions

Although ScanManipulator was created to address PITSI's data treatment requirements, it also includes functionalities to be used with MPISI. In this respect it automatically applies corrections and function fitting either to existing data files, or in near real time to data acquired directly from the neutron detector client software. The following procedures are currently available in ScanManipulator:

2.2.1. Flat field correction. Due to various physical factors such as gas pressure, delay line resistivity variations and variable pre-amplifier gains, area detectors rarely have homogeneous sensitivity throughout its whole surface area. This can be mitigated by performing a 'flat field' correction where the detector image pixel intensities are normalized using intensity data ($a_{i,j}$) from measurements of an isotropic scatterer such as vanadium. The relative sensitivity, s, of each pixel (i,j) is calculated as $s_{i,j} = a_{i,j} / max(a)$. During physical measurements, the corrected intensity of each pixel is calculated by dividing the detected intensity with the pixel's relative sensitivity.

2.2.2. Geometric correction. A Debye-Scherrer cone at 90° diffraction angle ($2\theta_{hkl}$) intersects the surface of an area detector as a straight line. Cones at any other angle intercept the detector as a curved line where the diffraction angle is only correct on the horizontal plane of the incident beam. Randau *et al.* has derived equations to reassign each pixel to a new coordinate that 'straightens' the curved lines to their corrected 2θ angle [8].

2.2.3. Integration. After application of the corrections, the two-dimensional frame is integrated vertically to produce a horizontal (one-dimensional) peak profile along the detector length. Conversion from linear length to subtention angle θ is done through calibration. Conversion of diffraction angle to d-spacing is achieved using the Bragg law with incorporation of the monochromatic wavelength.

2.2.4. Normalization. To negate variations in the incident neutron flux during the prolonged times (hours) involved in measuring a complete diffraction pattern, intensity data are normalized with respect to a 'beam monitor count' that is directly proportional to the flux experienced by the sample. A beam monitor is a low efficiency neutron detector placed in the primary monochromatic beam path.

2.2.5. Data cropping. Area detectors are inefficient close to the perimeter of the detection surface which results in a sharp falloff in reliability. Data in this region are subsequently excluded from analysis by removing marginal sections of the integrated data which represent the left and right extremes of the neutron detector frame dataset.

2.2.6. Data stitching. As discussed, it is often unlikely to have a single large area detector covering the whole 2θ range of interest. The range can be covered by step scanning detector arrays around the instrument rotation axis to produce partially overlapped detector frames. The frames are then combined to create a single continuous diffraction pattern. This procedure involves calculating the 2θ value of each detector channel with reference to the absolute 2θ value of detector center. From this, a common 2θ axis is created which spans the total measured range and each detector frame is interpolated onto it. Regions of overlap are identified and the average values for these areas used.

2.2.7. Sample edge determination. Entry curve routines as described by Brand [9] together with additional 'z-scan' and 'wall-scan' functions are used to determine the sample's relative position with respect to the gauge volume, which is defined by the overlap of the primary and secondary apertures.

2.2.8. Peak fitting. Data from MPISI and PITSI are used to determine diffraction peak parameters, such as peak center, peak intensity, integrated intensity, full-width-half maximum, background, etc. with associated uncertainties by fitting a Gaussian function to the corrected peak data.

2.3. Input and Output

ScanManipulator is able to input a variety of data formats which include a subset of the NeXus format [10] encoded with HDF5, data files originating from the McStas neutron ray-tracing simulation package [11] as well as two columns of ASCII. A dedicated module retrieves positional neutron data directly from the DAC system. This functionality allows automated peak fitting in real time which enables measurements according to pre-defined statistical criteria, instead of time.

Complete diffraction patterns can be exported to a FullProf [12] compatible format allowing quantitative phase analysis through Rietveld-refinement [13]. Peak fitting parameters can be exported to Microsoft Excel for processing. ScanManipulator exhibits a number of windows to facilitate visual display of datasets. These graphs can be copied to the clipboard in a txt, png, emf or bmp format.

3. Examples of data treatment functionalities and representations

ScanManipulator facilitates combining different diffraction pattern data sets as function of an instrument variable. Three examples are presented to indicate typical functionalities.

3.1. Temperature dependent phase transformation study on PITSI

As an example of grouping and visualization of temperature dependent data, the high temperature phase transformations in an alumina (Al_2O_3) sample have been investigated at 11 different temperatures using neutrons with a wavelength of 1.759 Å. At each constant temperature, a full diffraction pattern range composed of 7 detector frames each was measured. The measurement scheme shown in Figure 2 was applied that resulted in 77 datasets.

Data processing comprised applying all corrections for each detector frame and stitching into a continuous diffraction pattern. By setting the appropriate grouping parameter, data could automatically be picked and combined as function of temperature, giving 11 temperature datasets each containing a full diffraction pattern.

The diffraction results of Figure 3 indicate that a phase transformation had occurred at around 700 °C from a cubic to a hexagonal phase. In order to better identify the transition temperature, a representative Bragg peak, shown in Figure 4, was fitted with a Gaussian function. The fit was automatically applied to all datasets (temperatures) to compose the graph of Figure 5.

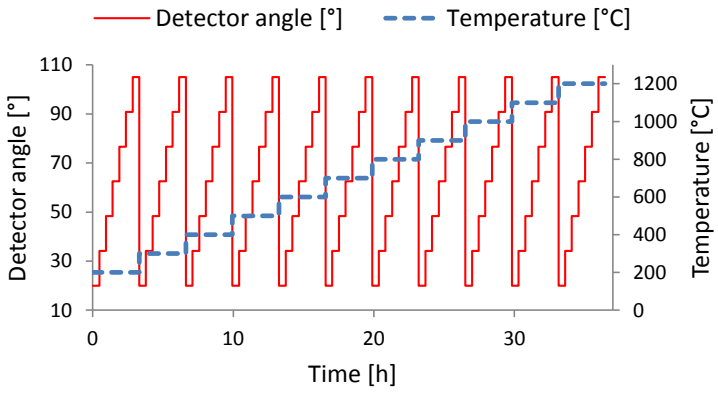

Figure 2. Graph showing the steps in detector angle and temperature versus time for a temperature dependant investigation.

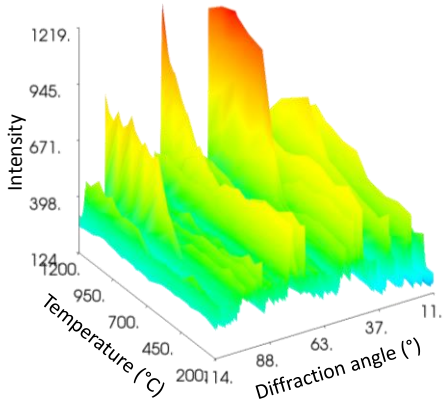

Figure 3. Waterfall plot showing diffraction pattern evolution as a function of temperature.

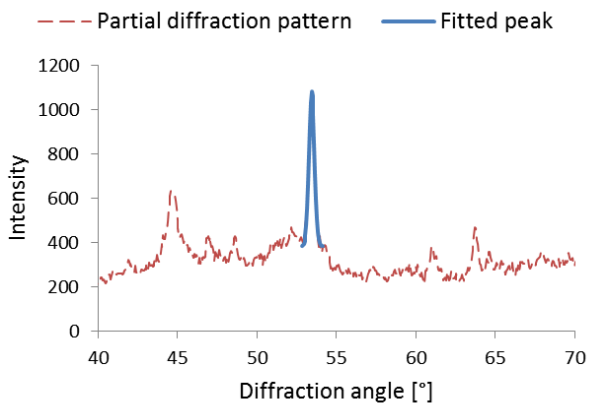

Figure 4. Diffraction pattern at 800 °C showing the peak at 2θ = 53.4° that was selected to follow its temperature dependence.

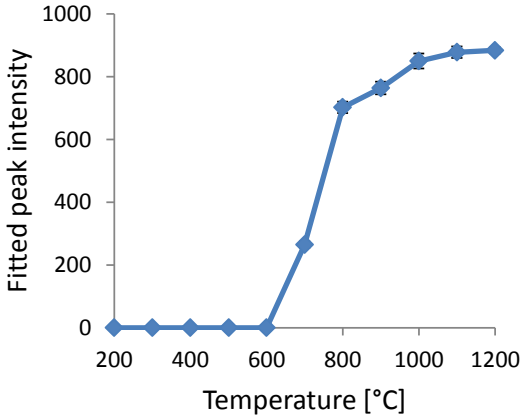

Figure 5. Graph showing the temperature dependence of the peak at 2θ = 53.4°.

3.2. Strain investigations on MPISI

Strain investigations of the interior regions of samples consist of measuring the depth and orientation dependence of a pre-selected diffraction peak. The peak angle is determined through Gaussian function fitting and is converted to d-spacing. Comparison of the d-values to an unstressed reference enables determination of the strain at that position and orientation. Figure 6 shows a typical sample setup on MPISI. By positioning the sample with respect to the gauge volume, cross-sections and even volumes of the sample can be investigated.

ScanManipulator performs the function fitting of multiple datasets automatically and exports results to Microsoft Excel where further calculations can be conducted. It can also be used as quick verification of multi-parameter trends for a specific strain direction setup as shown in Figure 7.

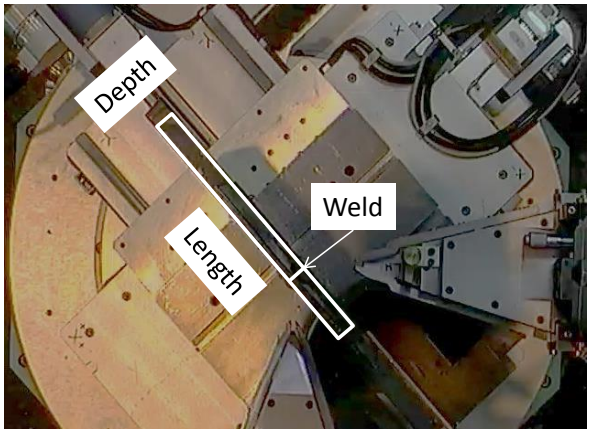

Figure 6. Photograph of a welded mild steel plate sample setup for measured on MPISI.

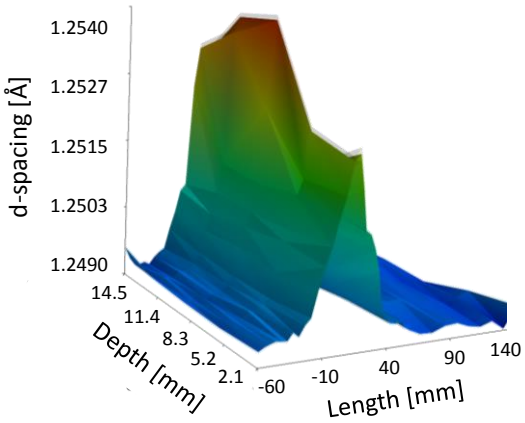

Figure 7. Graph showing the variation in (211) plane d-spacing in a welded mild steel sample as a function of multi-parameter positioning across the weld and plate depth.

3.3. Real-time peak fitting on MPISI

An instrument characterization investigation was conducted to determine the peak intensity count rate of the (211) peak of mild steel with respect to path length and gauge volume size. Figure 8 and Figure 9 summarize the multi-parameter results acquired using the real-time peak-fitting and evaluation functionality of ScanManipulator. Reaching of either of two conditions was specified, i.e. data acquisition to a maximum measurement time of 600s, or peak intensity of 40 counts. It can be seen that the required intensity could not be achieved for long path lengths with small gauge volumes within the allowed time. From the results it is evident that data acquisition against real-time evaluated set peak parameters is a viable process to be used in strain measurements.

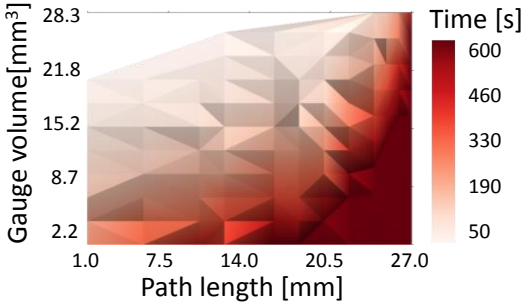

Figure 8. Surface plot showing measurement time as a function of gauge volume and path length.

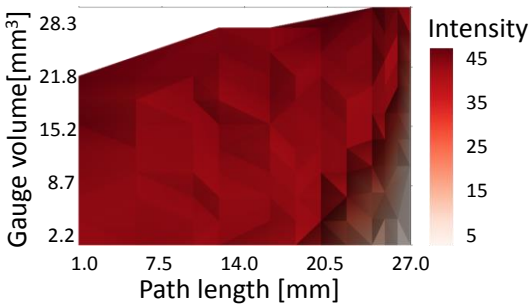

Figure 9. Surface plot showing fitted peak intensity as a function of gauge volume and path length.

4. Conclusion

A number of functionalities of ScanManipulator have been demonstrated. It provides a user friendly platform for users to automatically perform relevant corrections to neutron diffraction data originating from NDIFF instruments. Multi-parameter data can easily be displayed for visual interpretation and inspection.

Acknowledgements

This research is supported by the National Research Foundation of South Africa, grant number 84234, and Necsa SOC Limited. Any opinion, finding and conclusion or recommendation expressed in this material is that of the author(s) and the NRF does not accept any liability in this regard.

References

[1] Hugh Rayner H, Hathaway P, Hauser N, Fei Y, Franceschini F and Lam T 2006 *Physica* B **385-386** 1333-1335
[2] Arnold O *et al.* 2014 *Nucl Instrum Meth* A **764** 156-166
[3] Heer H, Könnecke M and Maden D 1998 *Physica* B **241-243** 124-126
[4] Wilkins S 2013 https://github.com/stuwilkins/pyspec Access date: 2014/05/06
[5] Collette A 2013 *Python and HDF5* (O'Reilly Media) pp 1-152
[6] Hunter J D 2007 *Comput Sci Eng* **9**(3) 90-95
[7] Ramachandran P and Varoquaux G 2011 *Comput Sci Eng* **13**(2) 40-51
[8] Randau C, Garbe U and Brokmeier H G 2011 *J. Appl. Cryst.* **44** 641-646
[9] Brand P C and Prask H J 1994 *J. Appl. Cryst* **27** 164-176
[10] Könnecke M *et al*. 2015 *J. Appl. Cryst.* **48** 301-305
[11] Lefmann K and Nielsen K 1999 *Neutron News* **10** 20
[12] Rodriguez-Carvajal J 1993 *Physica* B **192** 55-69
[13] Rietveld H M 1968 *J. Appl. Cryst.* **2** 65-71